Article

GdN@C (*n* = 40, 42, and 44): Remarkably Low HOMO–LUMO Gap and Unusual Electrochemical Reversibility of GdN@C

Manuel N. Chaur, Frederic Melin, Bevan Elliott, Andreas J. Athans, Kenneth Walker, Brian C. Holloway, and Luis Echegoyen

J. Am. Chem. Soc., **2007**, 129 (47), 14826-14829 • DOI: 10.1021/ja075930y

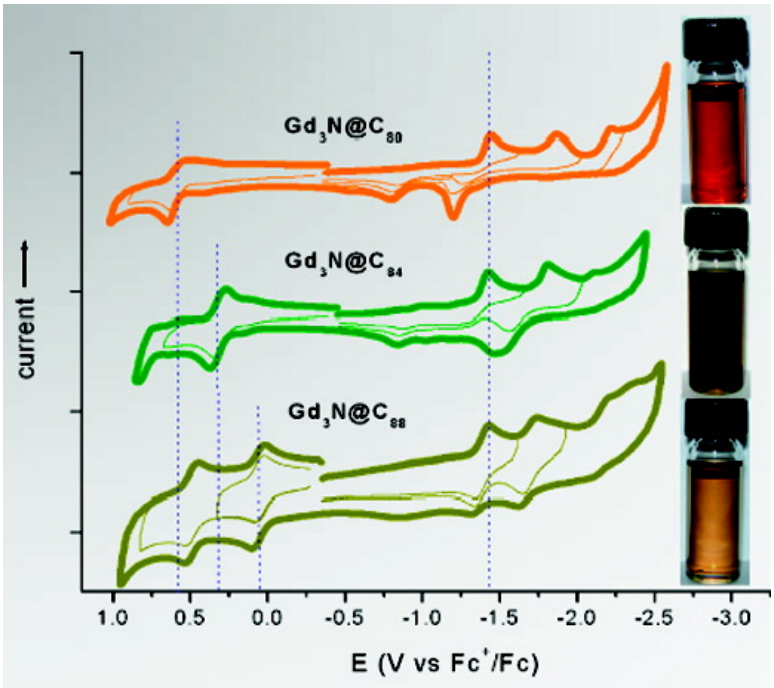

More About This Article

Additional resources and features associated with this article are available within the HTML version:

- Supporting Information
- Links to the 12 articles that cite this article, as of the time of this article download
- Access to high resolution figures
- Links to articles and content related to this article
- Copyright permission to reproduce figures and/or text from this article

J|A|C|S
ARTICLES
Published on Web 11/06/2007

$Gd_3N@C_{2n}$ ($n = 40$, 42, and 44): Remarkably Low HOMO−LUMO Gap and Unusual Electrochemical Reversibility of $Gd_3N@C_{88}$

Manuel N. Chaur,[†] Frederic Melin,[†] Bevan Elliott,[†] Andreas J. Athans,[†] Kenneth Walker,[‡] Brian C. Holloway,[‡] and Luis Echegoyen*,[†]

Contribution from the Department of Chemistry, Clemson University, Clemson, South Carolina 29634, and Luna Innovations, Inc. (nanoWorks division), 521 Bridge Street, Danville, Virginia 24541

Received August 7, 2007; E-mail: luis@clemson.edu

Abstract: High-performance liquid chromatography was used to isolate two new trimetallic nitride endohedral fullerenes, $Gd_3N@C_{2n}$ ($n = 42$ and 44), and they were characterized by MALDI-TOF mass spectrometry, UV−vis−NIR, and cyclic voltammetry. It was found that their electronic HOMO−LUMO gaps depend pronouncedly on the size of the cage, from a large band gap for $Gd_3N@C_{80}$ (2.02 V) to a small band gap for $Gd_3N@C_{88}$ (1.49 V). The electrochemical properties also change dramatically with the size of the cage, going from irreversible for the C_{80} cage to reversible for $Gd_3N@C_{88}$. The latter is the largest trimetallic cluster inside C_{88} isolated and characterized to date. $Gd_3N@C_{88}$ has one of the lowest electrochemical energy gaps for a nonderivatized metallofullerene.

Introduction

Since the discovery of the first trimetallic nitride template endohedral metallofullerene (TNT EMF) in 1999,[1] there has been great interest in these unique compounds because of their interesting chemical and physical properties and the many possibilities to prepare and isolate new kinds of metallofullerene-based materials.

The encapsulation of metal clusters inside fullerene cages is achieved by arc-burning graphite rods packed with metal oxides under a nitrogen source gas in a Krätschmer−Huffman reactor.[1] This process results in relatively low yields, thus making it difficult to prepare large enough quantities to characterize. The compounds are usually obtained as mixtures of $M_3N@C_{2n}$ ($38 \leq n \leq 44$) endohedral metallofullerenes, where $M_3N@C_{80}$ is typically the most abundant because of the intrinsic electronic stabilization between the cage and the cluster.[2] Higher endohedrals are always obtained simultaneously but usually in very small amounts, and their separation by high-performance liquid chromatography (HPLC) is difficult because of the production of several isomers of the same trimetallosphere with very close retention times.[3]

Lanthanide-based cluster fullerenes have shown great potential as contrast agents in magnetic resonance imaging. Gadolinium cluster fullerenes have already proven to have higher relaxivities than the commercial Gd^{3+} complexes currently in use,[4,5] and these results have enhanced the study of these metallofullerenes. Gd_3N is the largest cluster inside a C_{80} cage that has been isolated to date.[6] Krause and Dunsch[7] reported the formation of Gd_3N clusters inside cages as small as C_{80} and as large as C_{88}, but no isolation of the higher gadolinium endohedrals was reported. $Gd_3N@C_{80}$ is the most abundant trimetallic nitride endohedral isolated within the family, but it is also the lowest yielding material when compared to other metal clusters.[8−10] The redox properties of $M_3N@C_{80}$ (M = Sc, Y, Er, Tm, Dy)[12,13,15] have been reported, and they exhibit similar redox behavior consisting of two electrochemically irreversible reduction steps and one reversible oxidation step. No electrochemical studies have been reported to date for higher metallofullerenes, and thus nothing is known about the dependence of the redox properties on the size of the cage.

We report herein the isolation and electronic characterization of the $Gd_3N@C_{2n}$ ($n = 40$, 42, and 44) cluster fullerene family, including the first electrochemical study of higher endohedrals. It is also the first electrochemical study for the gadolinium

[†] Clemson University.
[‡] Luna Innovations, Inc.

(1) Stevenson, S.; Rice, G.; Glass, T.; Harich, K.; Cromer, F.; Jordan, M. R.; Craft, J.; Hajdu, E.; Bible, R.; Olmstead, M. M.; Maitra, K.; Fisher, A. J.; Balch, A. L.; Dorn, H. C. *Nature* **1999**, *401*, 55−57.
(2) Campanera, J. M.; Bo, C.; Poblet, J. M. *Angew. Chem., Int. Ed.* **2005**, *44*, 7230−7233.
(3) Dunsch, L.; Yang, S. *Phys. Chem. Chem. Phys.* **2007**, *9*, 3067−3081.
(4) Mikawa, M.; Kato, H.; Okumura, M.; Narataki, M.; Kanazawa, Y.; Miwa, N.; Shinohara, H. *Bioconjugate Chem.* **2001**, *12*, 510−514.
(5) Kato, H.; Kanazawa, Y.; Okumura, M.; Taninaka, A.; Yokawa, T.; Shinohara, H. *J. Am. Chem. Soc.* **2003**, *125*, 4391−4397.
(6) Stevenson, S.; Phillips, J. P.; Reid, J. E.; Olmstead, M. M.; Rath, S. P.; Balch, A. *Chem. Commun.* **2004**, *24*, 2814−2815.
(7) Krause, M.; Dunsch, L. *Angew. Chem., Int. Ed.* **2005**, *44*, 1557−1560.
(8) Zuo, T.; Beavers, C. M.; Duchamp, J. C.; Campbell, A.; Dorn, H. C.; Olmstead, M. M.; Balch, A. *J. Am. Chem. Soc.* **2007**, *129*, 2035−2043.
(9) Krause, M.; Wong, J.; Dunsch, L. *Chem.−Eur. J.* **2005**, *11*, 706−711.
(10) Yang, S.; Dunsch, L. *J. Phys. Chem. B* **2005**, *109*, 12320−12328.
(11) Dunsch, L.; Krause, M.; Noack, J.; Georgi, P. *J. Phys. Chem. Solids* **2004**, *65*, 309−315.
(12) Krause, M.; Liu, X.; Wong, J.; Pichler, T.; Knupfer, M.; Dunsch, L. *J. Phys. Chem. A* **2005**, *109*, 7088−7093.
(13) Yang, S.; Zalibera, M.; Rapta, P.; Dunsch, L. *Chem.−Eur. J.* **2006**, *12*, 7848−7855.
(14) Beavers, C. M.; Zuo, T.; Duchamp, J. C.; Harich, K.; Dorn, H. C.; Olmstead, M. M.; Balch, A. *J. Am. Chem. Soc.* **2006**, *128*, 11352−11353.
(15) Cardona, C. M.; Elliott, B.; Echegoyen, L. *J. Am. Chem. Soc.* **2006**, *128*, 6480−6485.

10.1021/ja075930y CCC: $37.00

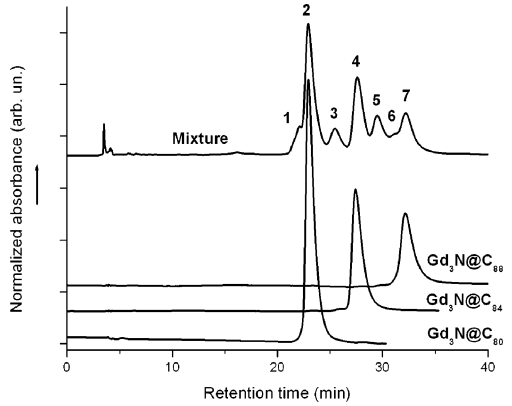

Figure 1. HPLC chromatograms of the $Gd_3N@C_{2n}$ mixture and isolated products.

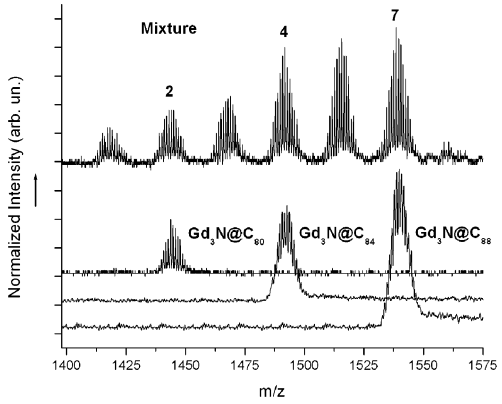

Figure 2. MALDI-TOF mass spectra of the $Gd_3N@C_{2n}$ mixture and the isolated products.

cluster fullerene family. We found that the electronic properties of these TNT EMFs change dramatically with the size of the cage as observed using cyclic voltammetry (CV). For the smaller cages (C_{80} and C_{84}), irreversible behavior is observed for the reduction steps, whereas for the highest cage isolated (C_{88}), we observed reversible electrochemistry in both oxidation and reduction steps. In addition, $Gd_3N@C_{88}$ exhibits the smallest electrochemical HOMO−LUMO gap within the series and the lowest of any endohedral metallofullerene studied to date.

Experimental Section

HPLC Separation of the $Gd_3N@C_{2n}$ Cluster Fullerenes Family. The material for this report was acquired by extracting all fullerene species, via solvent reflux, from the soot of a standard electric arc reactor[16] using graphite rods packed as previously described.[1] Empty cage fullerenes were removed by treating with cyclopentadiene as described before.[17,18] A mixture of higher order endohedral metallofullerenes and some $Gd_3N@C_{80}$ was separated from pure $Gd_3N@C_{80}$ via HPLC. The critical advantage to this study was the production volume at Luna Innovations (nanoWorks division), which allowed for the collection of a substantial amount of the very low yield species used in this study. Three fractions were successfully isolated from the $Gd_3N@C_{2n}$ ($39 \leq n \leq 44$) compounds by HPLC using a semipreparative 10 mm × 250 mm Buckyprep-M column.

Initially, the mixture showed seven peaks corresponding to the endohedrals with cages as small as C_{78} and as large as C_{88} (Figures 1 and 2), confirmed by matrix-assisted laser desorption/ionization time-of-flight mass spectrometry (MALDI-TOF). From this mixture, the isolation of peaks 2, 4, and 7, identified as $Gd_3N@C_{80}$, $Gd_3N@C_{84}$, and $Gd_3N@C_{88}$ according to their respective MALDI-TOF spectra (Figure 2), was possible, and the purity was higher than 95%. A further HPLC injection using a linear combination of a Buckyprep and a Buckyprep-M 10 mm × 250 mm columns with a flow rate of 1.60 mL/min was used as further evidence of isomeric purity (Supporting Information).

UV−Vis−NIR Studies of $Gd_3N@C_{2n}$ ($n = 40$, 42 and 44). Figure 3 shows the UV−vis−NIR spectra of the three isolated gadolinium metallofullerenes dissolved in toluene. The $Gd_3N@C_{80}$ HOMO−LUMO transitions are located at 705 and 675 nm with a spectral onset around 780 nm and a shoulder at 555 nm (Table 1). In the case of $Gd_3N@C_{84}$, an NIR absorption at 1089 nm with the HOMO−LUMO at 626 and 493 nm and its spectral onset around 1375 nm was present. These features reveal a small energy-gap electronic structure with a value (0.90 eV) below the limit between small and large band gap metallofullerenes. In the case of $Gd_3N@C_{88}$, its spectral onset was located around 1495 nm, which allowed us to calculate the energy gap as 0.83 eV. $Gd_3N@C_{88}$ also presents absorptions at 735, 546, 471, and 408 nm.

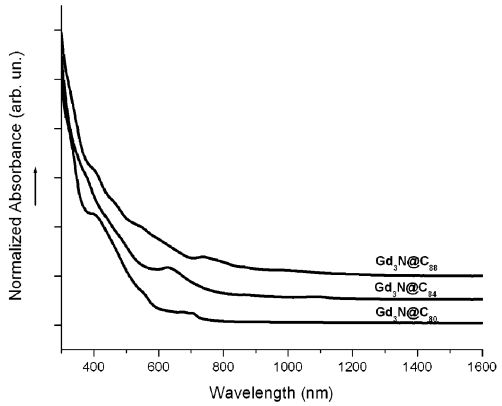

Figure 3. UV−vis−NIR spectra of $Gd_3N@C_{2n}$ ($n = 40$, 42, and 44) dissolved in toluene.

Table 1. Characteristic UV−Vis−NIR Absorptions and Absorption Onset of Some $M_3N@C_{2n}$ ($n = 40$, 42, and 44)

TNT EMF	onset (nm)	band gap (eV)[a]	UV–vis–NIR absorption peaks (nm)
$Gd_3N@C_{80}$ (I)	**780**	**1.60**	**407, 555, 675, 705**
$Tb_3N@C_{80}$ (I)	780	1.60	618, 643, 677, 707
$Dy_3N@C_{80}$ (I)	823	1.50	401, 554, 643, 670, 700
$Tm_3N@C_{80}$ (I)	780	1.60	407, 540, 675, 705
$Gd_3N@C_{84}$	**1375**	**0.90**	**378, 493, 626, 1089**
$Dy_3N@C_{84}$ (I)	1514	0.82	622, 870
$Dy_3N@C_{84}$ (II)	1485	0.84	374, 484, 625
$Tb_3N@C_{84}$ (II)			380, 468, 623
$Gd_3N@C_{88}$	**1495**	**0.83**	**408, 471, 546, 735**
$Tb_3N@C_{88}$			420, 480, 550, 758

[a] Band gap calculated from the spectral onset; band gap (eV) ≈ 1240/onset (nm).[10]

Electrochemical Studies of $Gd_3N@C_{2n}$ ($n = 40$, 42, and 44). Cyclic voltammetry of $Gd_3N@C_{80}$, $Gd_3N@C_{84}$, and $Gd_3N@C_{88}$ was performed in *o*-dichlorobenzene containing 0.05 M NBu_4PF_6 as supporting electrolyte, using a 3-mm-diameter glassy carbon disk as the working electrode. Ferrocene was added at the end of the experiments and used as an internal reference for measuring the potentials.

The CV of $Gd_3N@C_{80}$ at a scan rate of 100 mV/s showed three irreversible reduction processes and a reversible oxidation step (Figure

(16) Krätschmer, W.; Fostiropoulos, K.; Huffman, D. R. *Chem. Phys. Lett.* **1990**, *170*, 167−170.
(17) Ge, Z.; Duchamp, J. C.; Cai, T.; Gibson, H. W.; Dorn, H. C. *J. Am. Chem. Soc.* **2005**, *127*, 16292−16298.
(18) Stevenson, S.; Harich, K.; Yu, H.; Stephen, R. R.; Heaps, D.; Coumbe, C.; Phillips, J. P. *J. Am. Chem. Soc.* **2006**, *128*, 8829−8835.
(19) *CRC Handbook of Chemistry and Physics*, 81st ed.; Lide, D. R., Ed.; CRC Press: Boca Raton, FL, 2000.

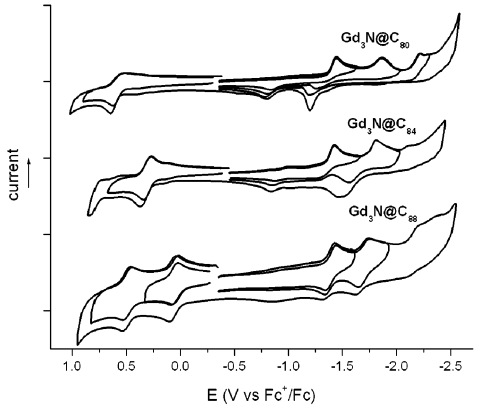

Figure 4. Cyclic voltammograms of $Gd_3N@C_{2n}$ (n = 40, 42, and 44) in NBu_4PF_6/*o*-DCB with ferrocene as the internal standard, 100 mV s^{-1} scan rate.

Table 2. Electronegativity and Redox Potentials (V vs Fc^+/Fc) of the $M_3N@C_{80}$ Cluster Fullerenes in *o*-DCB

		redox potential			
TNT EMF	χ^a	$E_{p,red(1)}$	$E_{p,red(2)}$	$E_{p,red(3)}$	$E_{1/2,ox(1)}$
$Gd_3N@C_{80}$ (I)	1.20	−1.44	−1.86	−2.18	+0.58
$Dy_3N@C_{80}$ (I)	1.22	−1.37	−1.86		+0.70
$Tm_3N@C_{80}$ (I)	1.25	−1.34	−1.78		+0.68
$Sc_3N@C_{80}$ (I)	1.36	−1.24	−1.62		+0.62

[a] Pauling electronegativity.[19]

4). On the basis of the first oxidation and first reduction steps, we calculated the electrochemical energy gap to be 2.02 V. When compared to other $M_3N@C_{80}$ (M = Dy, Tm, and Sc) endohedrals, it is quite similar, though larger than that of Sc (Table 2). Increasing the scan rates from 100 mV s^{-1} to 5 V s^{-1} did not improve the reversibility of reduction waves (Figure 5).

The electrochemistry of $Gd_3N@C_{84}$ was very similar to that of $Gd_3N@C_{80}$, with two irreversible reduction steps and a reversible oxidation step. However, both the reduction and oxidation steps were easier than that for $Gd_3N@C_{80}$, confirming the smaller HOMO−LUMO gap observed in the UV−visible spectrum. Scanning at faster scan rates from 100 mV s^{-1} to 2 V s^{-1} did not improve the reversibility of the reduction steps, similar to what was observed for $Gd_3N@C_{80}$ (Figure 6).

Surprisingly, $Gd_3N@C_{88}$ exhibited two reversible reduction steps and two reversible oxidation steps. Some additional reduction steps close to the solvent electrolyte potential window limit could also be observed, but these were not well defined. The first reduction potential was comparable to those of the smaller cages, but the first oxidation was shifted considerably to more negative values, making it much easier to oxidize than $Gd_3N@C_{80}$. This very low oxidation process indicates a considerably lower HOMO−LUMO gap of 1.49 V.

Results and Discussion

It has been known that endohedral metallofullerenes exhibit absorptions that are mainly due to $\pi-\pi^*$ transitions on the carbon cage and these depend on the structure and charge of the cage.[11] The UV−vis−NIR absorptions of the $Gd_3N@C_{2n}$ (n = 40, 42, and 44) cluster fullerene family were studied, and these showed similar absorption peaks as already reported for the I_h isomer[7] as well as for $Tm_3N@C_{80}$ (I).[9] These peaks also correlate fairly well with the absorptions of the I_h isomers of $Tb_3N@C_{80}$ and $Dy_3N@C_{80}$ (Table 1).[8,10] The data obtained for $Gd_3N@C_{84}$ correlate quite well with the absorptions observed for isomer (II) of $Dy_3N@C_{84}$[10] and with the UV−vis peaks reported for the non-IPR $Tb_3N@C_{84}$ (II) isomer.[14] In the case

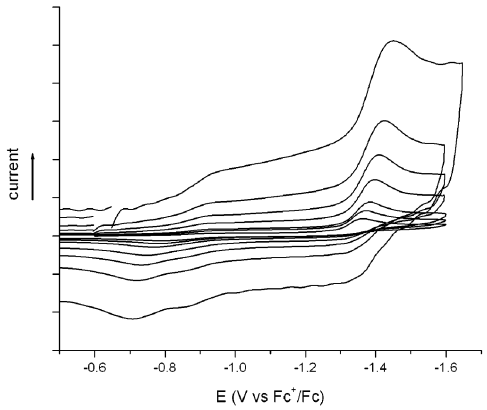

Figure 5. CV scan rate study of the first reduction wave of $Gd_3N@C_{80}$ (I). Scan rates of 50, 100, 200, 500, 1000, 2000, and 5000 mV s^{-1}.

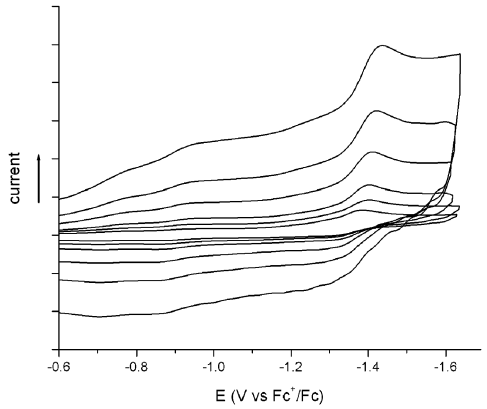

Figure 6. CV scan rate study of the first reduction wave of $Gd_3N@C_{84}$. Scan rates of 50, 100, 200, 500, 1000, and 2000 mV s^{-1}.

of $Gd_3N@C_{88}$, the absorption onset and the absorption peaks are well correlated with those found for $Tb_3N@C_{88}$.[8]

From the UV−vis−NIR data, it can be seen that the band gap of $Gd_3N@C_{2n}$ fullerenes decreases with increasing cage size, going from the large band gap in $Gd_3N@C_{80}$ (1.59 eV) to the smaller values for $Gd_3N@C_{84}$ and $Gd_3N@C_{88}$ (0.90 and 0.83 eV, respectively). Also, the similarity between the UV−vis absorption peaks of $Gd_3N@C_{84}$ with those observed for isomers (II) of $Dy_3N@C_{84}$ and $Tb_3N@C_{84}$ strongly suggests that the symmetry of the cage corresponds to the same non-IPR isomer with C_s symmetry.[14] In addition, the strong similarity between the absorption peaks of $Gd_3N@C_{88}$ and those reported for $Tb_3N@C_{88}$ suggests that the cage has D_2 symmetry, as reported for the latter.[8] However, the final cage symmetry assignments need to be confirmed by X-ray analysis, and those experiments are currently underway.

The peak potentials of the reduction steps for this family of TNTs seem to correlate well with the electronegativity of the encapsulated metal (Table 2). The TNT EMF that is easiest to reduce is also the one containing the most electronegative metal of the series (Sc), and the most difficult to reduce contains the least electronegative metal (Gd). This correlation is not as straightforward for the oxidation step, however, as $Gd_3N@C_{80}$ was found to be easier to oxidize than $Sc_3N@C_{80}$. This is probably an indication that the oxidation is based on the cage orbitals as opposed to those on the cluster, where reduction is based.[15]

Table 3. Redox Potentials (V vs Fc^+/Fc) and Electrochemical Energy Gap $\Delta E_{gap,ec}$ (V) of the $Gd_3N@C_{80}$ Cluster Fullerenes in NBu_4PF_6/*o*-DCB

	redox potential							
TNT EMF	$E_{p,red(1)}$	$E_{1/2,red(1)}$	$E_{p,red(2)}$	$E_{1/2,red(2)}$	$E_{p,red(3)}$	$E_{1/2,ox1}$	$E_{1/2,ox1}$	ΔE_{gap}
$Gd_3N@C_{80}$	−1.44		−1.86		−2.15	+0.58		2.02
$Gd_3N@C_{84}$	−1.37		−1.76			+0.32		1.69
$Gd_3N@C_{88}$	−1.43	−1.38	−1.74	−1.69		+0.06	+0.49	1.49

$Gd_3N@C_{88}$ showed interesting and unexpected redox properties with a very low reversible first oxidation step and with two reversible reduction steps at low scan rates, opening a promising way for future potential applications.

When looking at the energy gaps of these endohedrals (Table 3), it is also interesting to note that the main effect on the HOMO−LUMO gap arises as a consequence of the ease of the first oxidation with increasing cage size, going from 0.58 V for $Gd_3N@C_{80}$ to 0.32 V for $Gd_3N@C_{84}$ and finally to a very easily oxidized $Gd_3N@C_{88}$ cage at 0.06 V. While the size of the cage significantly affects the potential of the oxidation step in this series of $Gd_3N@C_{2n}$, it has almost no influence on the potential of the first reduction step. This makes sense since the reduction is based on the cluster, which is the same for all compounds, while the oxidation is based on the cage, which is pronouncedly different in all cases.

Conclusion

We have described the isolation and purification of the $Gd_3N@C_{2n}$ ($n = 40, 42, 44$) cluster metallofullerene family for the first time. These metallofullerenes were characterized by MALDI-TOF, UV−vis, and electrochemistry. Cyclic voltammetry showed that for $Gd_3N@C_{80}$ and $Gd_3N@C_{84}$ the reduction steps are irreversible and the oxidation steps reversible. Additionally and more importantly, we reported the first example of reversible electrochemistry for a TNT EMF, $Gd_3N@C_{88}$. A pronounced decrease of the HOMO−LUMO gap was observed, where the order is $Gd_3N@C_{80} > Gd_3N@C_{84} > Gd_3N@C_{88}$. Finally, we observed that the cage size affects the potential of the oxidation step in the electrochemistry but has essentially no effect on the first reduction.

Acknowledgment. We gratefully acknowledge Luna Innovations, Inc. for supplying us with $Gd_3N@C_{2n}$. Financial support from the National Science Foundation to A.J.A. and L.E. (Grant No. CHE-0509989) is greatly appreciated. This material is based on work supported by the National Science Foundation while L.E. was working there. This material was also based upon work supported by Luna Innovations and the Air Force Office of Scientific Research (AFOSR) under Contract No. FA9550-06-C-0010.

Supporting Information Available: HPLC chromatograms of isolated $Gd_3N@C_{84}$ and $Gd_3N@C_{88}$, UV−vis−NIR spectra for $Gd_3N@C_{84}$ and $Gd_3N@C_{88}$, as well as a photo of the three described $Gd_3N@C_{2n}$ fullerenes dissolved in toluene. This material is available free of charge via the Internet at http://pubs.acs.org.

JA075930Y